

# Overcoming catastrophic forgetting in neural networks

James Kirkpatrick<sup>a</sup>, Razvan Pascanu<sup>a</sup>, Neil Rabinowitz<sup>a</sup>, Joel Veness<sup>a</sup>, Guillaume Desjardins<sup>a</sup>, Andrei A. Rusu<sup>a</sup>, Kieran Milan<sup>a</sup>, John Quan<sup>a</sup>, Tiago Ramalho<sup>a</sup>, Agnieszka Grabska-Barwinska<sup>a</sup>, Demis Hassabis<sup>a</sup>, Claudia Clopath<sup>b</sup>, Dhharshan Kumaran<sup>a</sup>, and Raia Hadsell<sup>a</sup>

<sup>a</sup>DeepMind, London, N1C 4AG, United Kingdom

<sup>b</sup>Bioengineering department, Imperial College London, SW7 2AZ, London, United Kingdom

## Abstract

The ability to learn tasks in a sequential fashion is crucial to the development of artificial intelligence. Neural networks are not, in general, capable of this and it has been widely thought that *catastrophic forgetting* is an inevitable feature of connectionist models. We show that it is possible to overcome this limitation and train networks that can maintain expertise on tasks which they have not experienced for a long time. Our approach remembers old tasks by selectively slowing down learning on the weights important for those tasks. We demonstrate our approach is scalable and effective by solving a set of classification tasks based on the MNIST hand written digit dataset and by learning several Atari 2600 games sequentially.

## 1 Introduction

Achieving artificial general intelligence requires that agents are able to learn and remember many different tasks Legg and Hutter [2007]. This is particularly difficult in real-world settings: the sequence of tasks may not be explicitly labelled, tasks may switch unpredictably, and any individual task may not recur for long time intervals. Critically, therefore, intelligent agents must demonstrate a capacity for *continual learning*: that is, the ability to learn consecutive tasks without forgetting how to perform previously trained tasks.

Continual learning poses particular challenges for artificial neural networks due to the tendency for knowledge of previously learnt task(s) (e.g. task A) to be abruptly lost as information relevant to the current task (e.g. task B) is incorporated. This phenomenon, termed *catastrophic forgetting* [French, 1999, McCloskey and Cohen, 1989, McClelland et al., 1995, Ratcliff, 1990], occurs specifically when the network is trained sequentially on multiple tasks because the weights in the network that are important for task A are changed to meet the objectives of task B. Whilst recent advances in machine learning and in particular deep neural networks have resulted in impressive gains in performance across a variety of domains (e.g. [Krizhevsky et al., 2012, LeCun et al., 2015]), little progress has been made in achieving continual learning. Current approaches have typically ensured that data from all tasks are simultaneously available during training. By interleaving data from multiple tasks during learning, forgetting does not occur because the weights of the network can be jointly optimized for performance on all tasks. In this regime—often referred to as the *multitask learning* paradigm—deep learning techniques have been used to train single agents that can successfully play multiple Atari games [Rusu et al., 2015, Parisotto et al., 2015]. If tasks are presented sequentially, multitask learning can only be used if the data are recorded by an episodic memory system and replayed to the network during training. This approach (often called system-level consolidation [McClelland et al., 1995]), is impractical for learning large numbers of tasks, as in our setting it would require the amount of memories being stored and replayed to be proportional to the number of tasks. The lack of algorithms

to support continual learning thus remains a key barrier to the development of artificial general intelligence.

In marked contrast to artificial neural networks, humans and other animals appear to be able to learn in a continual fashion [Cichon and Gan, 2015]. Recent evidence suggests that the mammalian brain may avoid catastrophic forgetting by protecting previously-acquired knowledge in neocortical circuits [Cichon and Gan, 2015, Hayashi-Takagi et al., 2015, Yang et al., 2009, 2014]. When a mouse acquires a new skill, a proportion of excitatory synapses are strengthened; this manifests as an increase in the volume of individual dendritic spines of neurons [Yang et al., 2009]. Critically, these enlarged dendritic spines persist despite the subsequent learning of other tasks, accounting for retention of performance several months later [Yang et al., 2009]. When these spines are selectively “erased”, the corresponding skill is forgotten [Hayashi-Takagi et al., 2015, Cichon and Gan, 2015]. This provides causal evidence that neural mechanisms supporting the protection of these strengthened synapses are critical to retention of task performance. Together, these experimental findings—together with neurobiological models [Fusi et al., 2005, Benna and Fusi, 2016]—suggest that continual learning in the mammalian neocortex relies on a process of task-specific synaptic consolidation, whereby knowledge about how to perform a previously acquired task is durably encoded in a proportion of synapses that are rendered less plastic and therefore stable over long timescales.

In this work, we demonstrate that task-specific synaptic consolidation offers a novel solution to the continual learning problem for artificial intelligence. We develop an algorithm analogous to synaptic consolidation for artificial neural networks, which we refer to as *elastic weight consolidation* (EWC for short). This algorithm slows down learning on certain weights based on how important they are to previously seen tasks. We show how EWC can be used in supervised learning and reinforcement learning problems to train several tasks sequentially without forgetting older ones, in marked contrast to previous deep-learning techniques.

## 2 Elastic weight consolidation

In brains, synaptic consolidation enables continual learning by reducing the plasticity of synapses that are vital to previously learned tasks. We implement an algorithm that performs a similar operation in artificial neural networks by constraining important parameters to stay close to their old values. In this section we explain why we expect to find a solution to a new task in the neighbourhood of an older one, how we implement the constraint, and finally how we determine which parameters are important.

A deep neural network consists of multiple layers of linear projection followed by element-wise non-linearities. Learning a task consists of adjusting the set of weights and biases  $\theta$  of the linear projections, to optimize performance. Many configurations of  $\theta$  will result in the same performance [Nielsen, 1989, Sussmann, 1992]; this is relevant for EWC: over-parameterization makes it likely that there is a solution for task B,  $\theta_B^*$ , that is close to the previously found solution for task A,  $\theta_A^*$ . While learning task B, EWC therefore protects the performance in task A by constraining the parameters to stay in a region of low error for task A centered around  $\theta_A^*$ , as shown schematically in Figure 1. This constraint is implemented as a quadratic penalty, and can therefore be imagined as a spring anchoring the parameters to the previous solution, hence the name elastic. Importantly, the stiffness of this spring should not be the same for all parameters; rather, it should be greater for those parameters that matter most to the performance during task A.

In order to justify this choice of constraint and to define which weights are most important for a task, it is useful to consider neural network training from a probabilistic perspective. From this point of view, optimizing the parameters is tantamount to finding their most probable values given some data  $\mathcal{D}$ . We can compute this conditional probability  $p(\theta|\mathcal{D})$  from the prior probability of the parameters  $p(\theta)$  and the probability of the data  $p(\mathcal{D}|\theta)$  by using Bayes’ rule:

$$\log p(\theta|\mathcal{D}) = \log p(\mathcal{D}|\theta) + \log p(\theta) - \log p(\mathcal{D}) \quad (1)$$

Note that the log probability of the data given the parameters  $\log p(\mathcal{D}|\theta)$  is simply the negative of the loss function for the problem at hand  $-\mathcal{L}(\theta)$ . Assume that the data is split into two independent parts, one defining task A ( $\mathcal{D}_A$ ) and the other task B ( $\mathcal{D}_B$ ). Then, we can re-arrange equation 1:

$$\log p(\theta|\mathcal{D}) = \log p(\mathcal{D}_B|\theta) + \log p(\theta|\mathcal{D}_A) - \log p(\mathcal{D}_B) \quad (2)$$

Note that the left hand side is still describing the posterior probability of the parameters given the *entire* dataset, while the right hand side only depends on the loss function for task B  $\log p(\mathcal{D}_B|\theta)$ .

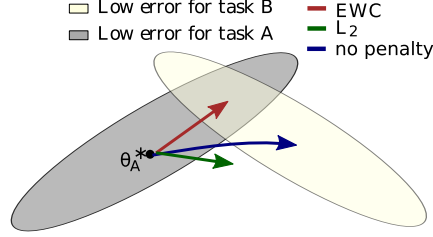


Figure 1: elastic weight consolidation (EWC) ensures task A is remembered whilst training on task B. Training trajectories are illustrated in a schematic parameter space, with parameter regions leading to good performance on task A (gray) and on task B (cream). After learning the first task, the parameters are at  $\theta_A^*$ . If we take gradient steps according to task B alone (blue arrow), we will minimize the loss of task B but destroy what we have learnt for task A. On the other hand, if we constrain each weight with the same coefficient (green arrow) the restriction imposed is too severe and we can only remember task A at the expense of not learning task B. EWC, conversely, finds a solution for task B without incurring a significant loss on task A (red arrow) by explicitly computing how important weights are for task A.

All the information about task A must therefore have been absorbed into the posterior distribution  $p(\theta|\mathcal{D}_A)$ . This posterior probability must contain information about which parameters were important to task A and is therefore the key to implementing EWC. The true posterior probability is intractable, so, following the work on the Laplace approximation by Mackay [MacKay, 1992], we approximate the posterior as a Gaussian distribution with mean given by the parameters  $\theta_A^*$  and a diagonal precision given by the diagonal of the Fisher information matrix  $F$ .  $F$  has three key properties [Pascanu and Bengio, 2013]: (a) it is equivalent to the second derivative of the loss near a minimum, (b) it can be computed from first-order derivatives alone and is thus easy to calculate even for large models, and (c) it is guaranteed to be positive semi-definite. Note that this approach is similar to expectation propagation where each subtask is seen as a factor of the posterior [Eskin et al., 2004]. Given this approximation, the function  $\mathcal{L}$  that we minimize in EWC is:

$$\mathcal{L}(\theta) = \mathcal{L}_B(\theta) + \sum_i \frac{\lambda}{2} F_i (\theta_i - \theta_{A,i}^*)^2 \quad (3)$$

where  $\mathcal{L}_B(\theta)$  is the loss for task B only,  $\lambda$  sets how important the old task is compared to the new one and  $i$  labels each parameter.

When moving to a third task, task C, EWC will try to keep the network parameters close to the learned parameters of both task A and B. This can be enforced either with two separate penalties, or as one by noting that the sum of two quadratic penalties is itself a quadratic penalty.

## 2.1 EWC allows continual learning in a supervised learning context

We start by addressing the problem of whether elastic weight consolidation could allow deep neural networks to learn a set of complex tasks without catastrophic forgetting. In particular, we trained a fully connected multilayer neural network on several supervised learning tasks in sequence. Within each task, we trained the neural network in the traditional way, namely by shuffling the data and processing it in small batches. After a fixed amount of training on each task, however, we allowed no further training on that task’s dataset.

We constructed the set of tasks from the problem of classifying hand written digits from the MNIST [LeCun et al., 1998] dataset, according to a scheme previously used in the continual learning literature [Srivastava et al., 2013, Goodfellow et al., 2014]. For each task, we generated a fixed, random permutation by which the input pixels of all images would be shuffled. Each task was thus of equal difficulty to the original MNIST problem, though a different solution would be required for each. Detailed description of the settings used can be found in Appendix 4.1.

Training on this sequence of tasks with plain stochastic gradient descent (SGD) incurs catastrophic forgetting, as demonstrated in Figure 2A. The blue curves show performance on the testing sets of two different tasks. At the point at which the training regime switches from training on the first task (A) to training on the second (B), the performance for task B falls rapidly, while for task A it climbs steeply. The forgetting of task A compounds further with more training time, and the addition

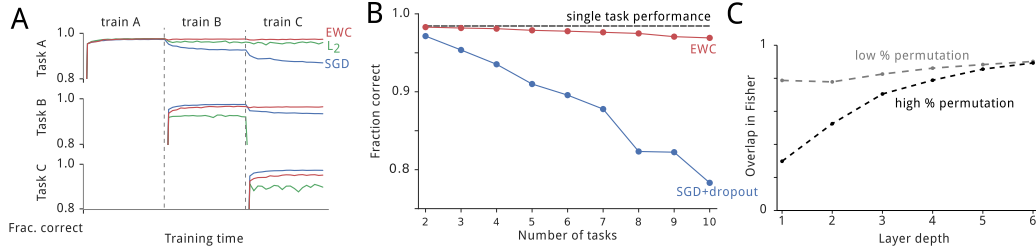


Figure 2: Results on the permuted MNIST task. A: Training curves for three random permutations A, B and C using EWC (red),  $L_2$  regularization (green) and plain SGD (blue). Note that only EWC is capable of maintaining a high performance on old tasks, while retaining the ability to learn new tasks. B: Average performance across all tasks using EWC (red) or SGD with dropout regularization (blue). The dashed line shows the performance on a single task only. C: Similarity between the Fisher information matrices as a function of network depth for two different amounts of permutation. Either a small square of 8x8 pixels in the middle of the image is permuted (grey) or a large square of 26x26 pixels is permuted (black). Note how the more different the tasks are, the smaller the overlap in Fisher information matrices in early layers.

of subsequent tasks. This problem cannot be countered by regularizing the network with a fixed quadratic constraint for each weight (green curves,  $L_2$  regularization): here, the performance in task A degrades much less severely, but task B cannot be learned properly as the constraint protects all weights equally, leaving little spare capacity for learning on B. However, when we use EWC, and thus take into account how important each weight is to task A, the network can learn task B well without forgetting task A (red curves). This is exactly the expected behaviour described diagrammatically in Figure 1.

Previous attempts to solve the continual learning problem for deep neural networks have relied upon careful choice of network hyperparameters, together with other standard regularization methods, in order to mitigate catastrophic forgetting. However, on this task, they have only achieved reasonable results on up to two random permutations [Srivastava et al., 2013, Goodfellow et al., 2014]. Using a similar cross-validated hyperparameter search as [Goodfellow et al., 2014], we compared traditional dropout regularization to EWC. We find that stochastic gradient descent with dropout regularization alone is limited, and that it does not scale to more tasks (Figure 2B). In contrast, EWC allows a large number of tasks to be learned in sequence, with only modest growth in the error rates.

Given that EWC allows the network to effectively squeeze in more functionality into a network with fixed capacity, we might ask whether it allocates completely separate parts of the network for each task, or whether capacity is used in a more efficient fashion by sharing representation. To assess this, we determined whether each task depends on the same sets of weights, by measuring the overlap between pairs of tasks’ respective Fisher information matrices (see Appendix 4.3). A small overlap means that the two tasks depend on different sets of weights (i.e. EWC subdivides the network’s weights for different tasks); a large overlap indicates that weights are being used for both the two tasks (i.e. EWC enables sharing of representations). Figure 2C shows the overlap as a function of depth. As a simple control, when a network is trained on two tasks which are very similar to each other (two versions of MNIST where only a few pixels are permuted), the tasks depend on similar sets of weights throughout the whole network (grey curve). When then the two tasks are more dissimilar from each other, the network begins to allocate separate capacity (i.e. weights) for the two tasks (black line). Nevertheless, even for the large permutations, the layers of the network closer to the output are indeed being reused for both tasks. This reflects the fact that the permutations make the input domain very different, but the output domain (i.e. the class labels) is shared.

## 2.2 EWC allows continual learning in a reinforcement learning context

We next tested whether elastic weight consolidation could support continual learning in the far more demanding reinforcement learning (RL) domain. In RL, agents dynamically interact with the environment in order to develop a policy that maximizes cumulative future reward. We asked whether Deep Q Networks (DQNs)—an architecture that has achieved impressive successes in such challenging RL settings [Mnih et al., 2015]—could be harnessed with EWC to successfully support continual learning in the classic Atari 2600 task set [Bellemare et al., 2013]. Specifically, each

experiment consisted of ten games chosen randomly from those that are played at human level or above by DQN. At training time, the agent was exposed to experiences from each game for extended periods of time. The order of presentation of the games was randomized and allowed for returning to the same games several times. At regular intervals we would also test the agent’s score on each of the ten games, without allowing the agent to train on them (Figure 3A).

Notably, previous reinforcement learning approaches to continual learning have either relied on either adding capacity to the network [Ring, 1998, Rusu et al., 2016] or on learning each task in separate networks, which are then used to train a single network that can play all games [Rusu et al., 2015, Parisotto et al., 2015]. In contrast, the EWC approach presented here makes use of a single network with fixed resources (i.e. network capacity) and has minimal computational overhead.

In addition to using EWC to protect previously-acquired knowledge, we used the RL domain to address a broader set of requirements that are needed for successful continual learning systems: in particular, higher-level mechanisms are needed to infer which task is currently being performed, detect and incorporate novel tasks as they are encountered, and allow for rapid and flexible switching between tasks [Collins and Frank, 2013]. In the primate brain, the prefrontal cortex is widely viewed as supporting these capabilities by sustaining neural representations of task context that exert top-down gating influences on sensory processing, working memory, and action selection in lower-level regions [O’Reilly and Frank, 2006, Mante et al., 2013, Miller and Cohen, 2001, Doya et al., 2002].

Inspired by this evidence, we used an agent very similar to that described in [van Hasselt et al., 2016] with few differences: (a) a network with more parameters, (b) a smaller transition table, (c) task-specific bias and gains at each layer, (d) the full action set in Atari, (e) a task-recognition model, and (f) the EWC penalty. Full details of hyper-parameters are described in Appendix *app:atari*. Here we briefly describe the two most important modifications to the agent: the task-recognition module, and the implementation of the EWC penalty.

We treat the task context as the latent variable of a Hidden Markov Model. Each task is therefore associated to an underlying generative model of the observations. The main distinguishing feature of our approach is that we allow for the addition of new generative models if they explain recent data better than the existing pool of models by using a training procedure inspired by the forget me not process [Kieran et al., 2016] (see Appendix 4.2).

In order to apply EWC, we compute the Fisher information matrix at each task switch. For each task, a penalty is added with anchor point given by the current value of the parameters and with weights given by the Fisher information matrix times a scaling factor  $\lambda$  which was optimized by hyperparameter search. We only added an EWC penalty to games which had experienced at least 20 million frames.

We also allowed the DQN agents to maintain separate short-term memory buffers for each inferred task: these allow action values for each task to be learned off-policy using an experience replay mechanism [Mnih et al., 2015]. As such, the overall system has memory on two time-scales: over short time-scales, the experience replay mechanism allows learning in DQN to be based on the interleaved and uncorrelated experiences [Mnih et al., 2015]. At longer time scales, know-how across tasks is consolidated by using EWC. Finally, we allowed a small number of network parameters to be game-specific, rather than shared across games. In particular, we allowed each layer of the network to have biases and per element multiplicative gains that were specific to each game.

We compare the performance of agents which use EWC (red) with ones that do not (blue) over sets of ten games in Figure 3. We measure the performance as the total human-normalized score across all ten games. We average across random seeds and over the choice of which ten games were played (see Appendix 4.2). We also clip the human-normalized score for each game to 1. Our measure of performance is therefore a number with a maximum of 10 (at least at human level on all games) where 0 means the agent is as good as a random agent. If we rely on plain gradient descent methods as in [Mnih et al., 2015], the agent never learns to play more than one game and the harm inflicted by forgetting the old games means that the total human-normalized score remains below one. By using EWC, however, the agents do indeed learn to play multiple games. As a control, we also considered the benefit to the agent if we explicitly provided the agent with the true task label (Figure 3B, brown), rather than relying on the learned task recognition through the FMN algorithm (red). The improvement here was only modest.

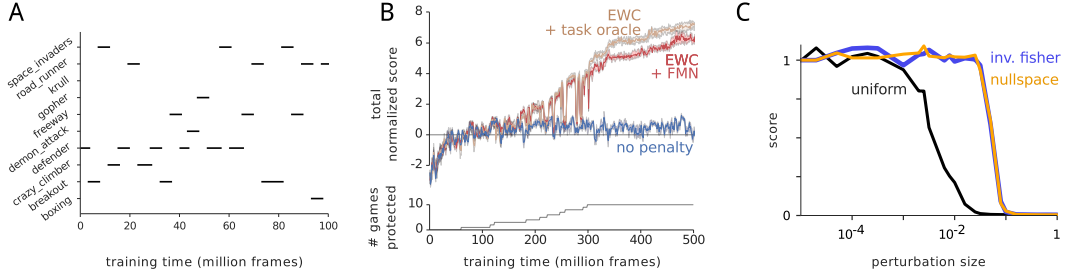


Figure 3: Results on Atari task. A: Schedule of games. Black bars indicate the sequential training periods (segments) for each game. After each training segment, performance on all games is measured. The EWC constraint is only activated to protect an agent’s performance on each game once the agent has experienced 20 million frames in that game. B: Total scores for each method across all games. Red curve denotes the network which infers the task labels using the Forget Me Not algorithm; brown curve is the network provided with the task labels. The EWC and SGD curves start diverging when games start being played again that have been protected by EWC. C: Sensitivity of a single-game DQN, trained on Breakout, to noise added to its weights. The performance on Breakout is shown as a function of the magnitude (standard deviation) of the weight perturbation. The weight perturbation is drawn from a zero mean Gaussian with covariance that is either uniform (black; i.e. targets all weights equally), the inverse Fisher ( $(F + \lambda I)^{-1}$ ; blue; i.e. mimicking weight changes allowed by EWC), or uniform within the nullspace of the Fisher (orange; i.e. targets weights that the Fisher estimates that the network output is entirely invariant to). To evaluate the score, we ran the agent for ten full game episodes, drawing a new random weight perturbation for every timestep.

While augmenting the DQN agent with EWC allows it to learn many games in sequence without suffering from catastrophic forgetting, it does not reach the score that would have been obtained by training ten separate DQNs (see Figure 1 in Appendix 4.2). One possible reason for this is that we consolidated weights for each game based on a tractable approximation of parameter uncertainty, the Fisher Information. We therefore sought to test the quality of our estimates empirically. To do so, we trained an agent on a single game, and measured how perturbing the network parameters affected the agent’s score. Regardless of which game the agent was trained on, we observed the same patterns, shown in Figure 3C. First, the agent was always more robust to parameter perturbations shaped by the inverse of the diagonal of the Fisher Information (blue), as opposed to uniform perturbations (black). This validates that the diagonal of the Fisher is a good estimate of how important a certain parameter is. Within our approximation, perturbing in the nullspace should have no effect on performance at all on performance. Empirically, however, we observe that perturbing in this space (orange) has the same effect as perturbing in the inverse Fisher space. This suggests that we are over-confident about certain parameters being unimportant: it is therefore likely that the chief limitation of the current implementation is that it under-estimates parameter uncertainty.

### 3 Discussion

We present a novel algorithm, elastic weight consolidation, that addresses the significant problem continual learning poses for neural networks. EWC allows knowledge of previous tasks to be protected during new learning, thereby avoiding catastrophic forgetting of old abilities. It does so by selectively decreasing the plasticity of weights, and thus has parallels with neurobiological models of synaptic consolidation. We implement EWC as a soft, quadratic constraint whereby each weight is pulled back towards its old values by an amount proportional to its importance for performance on previously-learned tasks. To the extent that tasks share structure, networks trained with EWC reuse shared components of the network. We further show that EWC can be effectively combined with deep neural networks to support continual learning in challenging reinforcement learning scenarios, such as Atari 2600 games.

The EWC algorithm can be grounded in Bayesian approaches to learning. Formally, when there is a new task to be learnt, the network parameters are tempered by a prior which is the *posterior* distribution on the parameters given data from previous task(s). This enables fast learning rates on parameters that are poorly constrained by the previous tasks, and slow learning rates for those which are crucial.

There has been previous work [French and Chater, 2002, Eaton and Ruvolo, 2013] using a quadratic penalty to approximate old parts of the dataset, but these applications have been limited to small models. Specifically, [French and Chater, 2002] used random inputs to compute a quadratic approximation to the energy surface. Their approach is slow, as it requires re-computing the curvature at each sample. The ELLA algorithm described in [Eaton and Ruvolo, 2013] requires computing and inverting matrices with a dimensionality equal to the number of parameters being optimized, therefore it has been mainly applied to linear and logistic regressions. In contrast, EWC has a run time which is linear in both the number of parameters and the number of training examples. We could only achieve this low computational complexity by making several simplifications, most notably by approximating the posterior distribution of the parameters on a task (i.e. the weight uncertainties) by a factorized Gaussian, and by computing its variance using a point-estimate of the parameters, via the diagonal of the Fisher Information matrix. Despite its low computational cost and empirical successes—even in the setting of challenging RL domains—our use of a point estimate of the posterior’s variance (as in a Laplace approximation) does constitute a significant weakness (see Fig 4C). Our initial explorations suggest that one might improve on this local estimate by using Bayesian neural networks [Blundell et al., 2015].

While this paper has primarily focused on building an algorithm out of neurobiological observations, it is also instructive to consider whether the algorithm’s successes can feed back into our understanding of the brain. In particular, we see considerable parallels between EWC and two computational theories of synaptic plasticity.

In this respect, the perspective we offer here aligns with a recent proposal that each synapse not only stores its current weight, but also an implicit representation of its uncertainty about that weight [Aitchison and Latham, 2015]. This idea is grounded in observations that post-synaptic potentials are highly variable in amplitude (suggestive of sampling from the weight posterior during computation), and that those synapses which are more variable are more amenable to potentiation or depression (suggestive of updating the weight posterior). While we do not explore the computational benefits of sampling from a posterior here, our work aligns with the notion that weight uncertainty should inform learning rates. We take this one step further, to emphasize that consolidating the high precision weights enables continual learning over long time scales. With EWC, three values have to be stored for each synapse: the weight itself, its variance and its mean. Interestingly, synapses in the brain also carry more than one piece of information. For example, the state of the short-term plasticity could carry information on the variance [Aitchison and Latham, 2015, Pfister et al., 2010]. The weight for the early phase of plasticity [Clopath et al., 2008] could encode the current synaptic strength, whereas the weight associated with the late-phase of plasticity or the consolidated phase could encode the mean weight.

The ability to learn tasks in succession without forgetting is a core component of biological and artificial intelligence. In this work we show that an algorithm that supports continual learning—which takes inspiration from neurobiological models of synaptic consolidation—can be combined with deep neural networks to achieve successful performance in a range of challenging domains. In doing so, we demonstrate that current neurobiological theories concerning synaptic consolidation do indeed scale to large-scale learning systems. This provides *prima facie* evidence that these principles may be fundamental aspects of learning and memory in the brain.

**Acknowledgements.** We would like to thank P. Dayan, D. Wierstra, S. Mohamed, Yee Whye Teh and K. Kavukcuoglu.

## References

- Laurence Aitchison and Peter E Latham. Synaptic sampling: A connection between psp variability and uncertainty explains neurophysiological observations. *arXiv preprint arXiv:1505.04544*, 2015.
- Marc G Bellemare, Yavar Naddaf, Joel Veness, and Michael Bowling. The arcade learning environment: An evaluation platform for general agents. *Journal of Artificial Intelligence Research*, 47: 253–279, 2013.
- Marcus K Benna and Stefano Fusi. Computational principles of synaptic memory consolidation. *Nature neuroscience*, 2016.

- Charles Blundell, Julien Cornebise, Koray Kavukcuoglu, and Daan Wierstra. Weight uncertainty in neural network. In *Proceedings of The 32nd International Conference on Machine Learning*, pages 1613–1622, 2015.
- Joseph Cichon and Wen-Biao Gan. Branch-specific dendritic  $ca^{2+}$  spikes cause persistent synaptic plasticity. *Nature*, 520(7546):180–185, 2015.
- Claudia Clopath, Lorric Ziegler, Eleni Vasilaki, Lars Büsing, and Wulfram Gerstner. Tag-trigger-consolidation: a model of early and late long-term-potential and depression. *PLoS Comput Biol*, 4(12):e1000248, 2008.
- Anne GE Collins and Michael J Frank. Cognitive control over learning: creating, clustering, and generalizing task-set structure. *Psychological review*, 120(1):190, 2013.
- DC Dowson and BV Landau. The fréchet distance between multivariate normal distributions. *Journal of multivariate analysis*, 12(3):450–455, 1982.
- Kenji Doya, Kazuyuki Samejima, Ken-ichi Katagiri, and Mitsuo Kawato. Multiple model-based reinforcement learning. *Neural computation*, 14(6):1347–1369, 2002.
- Eric Eaton and Paul L Ruvolo. Ella: An efficient lifelong learning algorithm. In *International Conference on Machine Learning*, pages 507–515, 2013.
- Eleazar Eskin, Alex J. Smola, and S.v.n. Vishwanathan. Laplace propagation. In *Advances in Neural Information Processing Systems 16*, pages 441–448. MIT Press, 2004. URL <http://papers.nips.cc/paper/2444-laplace-propagation.pdf>.
- Robert M French. Catastrophic forgetting in connectionist networks. *Trends in cognitive sciences*, 3(4):128–135, 1999.
- Robert M French and Nick Chater. Using noise to compute error surfaces in connectionist networks: a novel means of reducing catastrophic forgetting. *Neural computation*, 14(7):1755–1769, 2002.
- Stefano Fusi, Patrick J Drew, and LF Abbott. Cascade models of synaptically stored memories. *Neuron*, 45(4):599–611, 2005.
- Ian J Goodfellow, Mehdi Mirza, Da Xiao, Aaron Courville, and Yoshua Bengio. An empirical investigation of catastrophic forgetting in gradient-based neural networks. *Int’l Conf. on Learning Representations (ICLR)*, 2014.
- Akiko Hayashi-Takagi, Sho Yagishita, Mayumi Nakamura, Fukutoshi Shirai, Yi I. Wu, Amanda L. Loshbaugh, Brian Kuhlman, Klaus M. Hahn, and Haruo Kasai. Labelling and optical erasure of synaptic memory traces in the motor cortex. *Nature*, 525(7569):333–338, 09 2015. URL <http://dx.doi.org/10.1038/nature15257>.
- Milan Kieran, Joel Veness, Michael Bowling, James Kirkpatrick, Anna Koop, and Demis Hassabis. The forget me not process. In *Advances in Neural Information Processing Systems 26*, page accepted for publication, 2016.
- Alex Krizhevsky, Ilya Sutskever, and Geoffrey E Hinton. Imagenet classification with deep convolutional neural networks. In *NIPS*, pages 1097–1105, 2012.
- Yann LeCun, Corinna Cortes, and Christopher JC Burges. The mnist database of handwritten digits, 1998.
- Yann LeCun, Yoshua Bengio, and Geoffrey Hinton. Deep learning. *Nature*, 521(7553):436–444, 2015.
- Shane Legg and Marcus Hutter. Universal intelligence: A definition of machine intelligence. *Minds and Machines*, 17(4):391–444, 2007.
- David JC MacKay. A practical bayesian framework for backpropagation networks. *Neural computation*, 4(3):448–472, 1992.



- Valerio Mante, David Sussillo, Krishna V Shenoy, and William T Newsome. Context-dependent computation by recurrent dynamics in prefrontal cortex. *Nature*, 503(7474):78–84, 2013.
- James L McClelland, Bruce L McNaughton, and Randall C O’Reilly. Why there are complementary learning systems in the hippocampus and neocortex: insights from the successes and failures of connectionist models of learning and memory. *Psychological review*, 102(3):419, 1995.
- Michael McCloskey and Neal J Cohen. Catastrophic interference in connectionist networks: The sequential learning problem. *The psychology of learning and motivation*, 24(109-165):92, 1989.
- Earl K Miller and Jonathan D Cohen. An integrative theory of prefrontal cortex function. *Annual review of neuroscience*, 24(1):167–202, 2001.
- Volodymyr Mnih, Koray Kavukcuoglu, David Silver, Andrei A Rusu, Joel Veness, Marc G Bellemare, Alex Graves, Martin Riedmiller, Andreas K Fidjeland, Georg Ostrovski, et al. Human-level control through deep reinforcement learning. *Nature*, 518(7540):529–533, 2015.
- Robert H. Nielsen. Theory of the backpropagation neural network. In *Proceedings of the International Joint Conference on Neural Networks*, volume I, pages 593–605. Piscataway, NJ: IEEE, 1989.
- Randall C O’Reilly and Michael J Frank. Making working memory work: a computational model of learning in the prefrontal cortex and basal ganglia. *Neural computation*, 18(2):283–328, 2006.
- Emilio Parisotto, Jimmy Lei Ba, and Ruslan Salakhutdinov. Actor-mimic: Deep multitask and transfer reinforcement learning. *arXiv preprint arXiv:1511.06342*, 2015.
- Razvan Pascanu and Yoshua Bengio. Revisiting natural gradient for deep networks. *arXiv preprint arXiv:1301.3584*, 2013.
- Jean-Pascal Pfister, Peter Dayan, and Máté Lengyel. Synapses with short-term plasticity are optimal estimators of presynaptic membrane potentials. *Nature neuroscience*, 13(10):1271–1275, 2010.
- Roger Ratcliff. Connectionist models of recognition memory: constraints imposed by learning and forgetting functions. *Psychological review*, 97(2):285, 1990.
- Mark B Ring. Child: A first step towards continual learning. In *Learning to learn*, pages 261–292. Springer, 1998.
- Andrei A Rusu, Sergio Gomez Colmenarejo, Caglar Gulcehre, Guillaume Desjardins, James Kirkpatrick, Razvan Pascanu, Volodymyr Mnih, Koray Kavukcuoglu, and Raia Hadsell. Policy distillation. *arXiv preprint arXiv:1511.06295*, 2015.
- Andrei A Rusu, Neil C Rabinowitz, Guillaume Desjardins, Hubert Soyer, James Kirkpatrick, Koray Kavukcuoglu, Razvan Pascanu, and Raia Hadsell. Progressive neural networks. *arXiv preprint arXiv:1606.04671*, 2016.
- Rupesh K Srivastava, Jonathan Masci, Sohrab Kazerounian, Faustino Gomez, and Juergen Schmidhuber. Compete to compute. In *Advances in Neural Information Processing Systems 26*, pages 2310–2318. Curran Associates, Inc., 2013. URL <http://papers.nips.cc/paper/5059-competeto-compute.pdf>.
- Héctor J. Sussmann. Uniqueness of the weights for minimal feedforward nets with a given input-output map. *Neural Networks*, 5:589–593, 1992.
- Hado van Hasselt, Arthur Guez, and David Silver. Deep reinforcement learning with double q-learning. *Proceedings of the Thirtieth AAAI Conference on Artificial Intelligence*, pages 2094–2100, 2016.
- Joel Veness, Kee Siong Ng, Marcus Hutter, and Michael Bowling. Context tree switching. In *2012 Data compression conference.*, pages 327–336. IEEE, 2012.
- Guang Yang, Feng Pan, and Wen-Biao Gan. Stably maintained dendritic spines are associated with lifelong memories. *Nature*, 462(7275):920–924, 2009.
- Guang Yang, Cora Sau Wan Lai, Joseph Cichon, Lei Ma, Wei Li, and Wen-Biao Gan. Sleep promotes branch-specific formation of dendritic spines after learning. *Science*, 344(6188):1173–1178, 2014.

Hyperparameter	Reference figure		
	3A	3B	3C
learning rate	$10^{-3}$	$10^{-5}$ - $10^{-3}$	$10^{-3}$
dropout	no	yes	no
early stopping	no	yes	no
n. hidden layers	2	2	6
width hidden layers	400	400-2000	100
epochs / dataset	20	100	100

Table 1: Hyperparameters for each of the MNIST figures

## 4 Appendix

### 4.1 MNIST experiments

We carried out all MNIST experiments with fully-connected networks with rectified linear units. In order to replicate the results of [Goodfellow et al., 2014], we compared to results obtained using dropout regularization. As suggested in [Goodfellow et al., 2014], we applied dropout with a probability of 0.2 to the input and of 0.5 to the other hidden layers. In order to give SGD with dropout the best possible chance, we also used early stopping. Early stopping was implemented by computing the test error on the validation set for all pixel permutations seen to date. Here, if the validation error was observed to increase for more than five subsequent steps, we terminated this training segment and proceeded to the next dataset; at this point, we reset the network weights to the values that had the lowest average validation error on all previous datasets. Table 1 shows a list of all hyperparameters used to produce the three graphs in Figure 3 of the main text. Where a range is present, the parameter was randomly varied and the reported results were obtained using the best hyperparameter setting. When random hyperparameter search was used, 50 combinations of parameters were attempted for each number experiment.

### 4.2 Atari experiments

The agent architecture used is almost identical to that used in [van Hasselt et al., 2016]. In this section we provide details on all the parameters used.

Images are preprocessed in the same way as in [Mnih et al., 2015], namely the 210x160 images from the Atari emulator are downsampled to 84x84 using bilinear interpolation. We then convert the RGB images to YUV and use the grayscale channel alone. The state used by the agent consists of the four latest downsampled, grayscale observations concatenated together.

The network structure used is similar to the one from [Mnih et al., 2015], namely three convolutional layers followed by a fully connected layer. The first convolution had kernel size 8, stride 4 and 32 filters. The second convolution had kernel size 4, stride 2 and 64 filters. The final convolution had kernels size 3, stride 1 and 128 filters. The fully connected layer had 1024 units. Note that this network has approximately four times as many parameters as the standard network, due to having twice as many fully connected units and twice as many filters in the final convolution. The other departure from the standard network is that each layer was allowed to have task-specific gains and biases. For each layer, the transformation  $x \rightarrow y$  computed by the network is therefore:

$$y_i = \left( \sum_j W_{ij} x_j + b_i^c \right) g_i^c \quad (4)$$

where the biases  $b$  and the gains  $g$ . The network weights and biases were initialized by setting them randomly with a uniform number between  $-\sigma$  and  $\sigma$ , with  $\sigma$  set to the square root of the incoming hidden units (for a linear layer) or set to the area of the kernel times the number of incoming filters (for convolutional layers). Biases and gains were initialized to 0 and 1 respectively.

We used an  $\epsilon$ -greedy exploration policy, where the probability of selecting random action,  $\epsilon$ , decayed with training time. We kept a different timer for each of the tasks. We set  $\epsilon = 1$  for  $5 \times 10^4$  time steps, and then decayed this linearly to a value of 0.01 for the next  $10^6$ .

We trained the networks with the Double Q-learning algorithm [van Hasselt et al., 2016]. A training step is carried out on a minibatch of 32 experiences every four steps. The target network is updated every  $3 \times 10^4$  time steps. We trained with RMSProp, with a momentum of 0., a decay of 0.95, a learning rate of  $2.5 \times 10^{-4}$ , and a maximum learning rate of  $2.5 \times 10^{-3}$ .

Other hyperparameters that we changed from the reference implementation were: 1) using a smaller replay buffer ( $5 \times 10^5$  past experiences), and 2) a scaling factor for the EWC penalty of 400. Another subtle difference is that we used the full action set in the Atari emulator. In fact, although many games only support a small subset of the 18 possible actions, in order to have a unified network structure for all games we used 18 actions in each game.

We randomly chose the 10 games for each experiment from a pool of 19 Atari games for which the standalone DQN could reach human-level performance in  $50 \times 10^6$  frames. The scores for each of these games for the baseline algorithm, for EWC and for plain SGD training, as a function of the number steps played *in that game* are shown in Figure 4. In order to get an averaged performance, we chose 10 sets of 10 games, and ran 4 different random seeds for each set.

The most significant departure from the published models is the automatic determination of the task. We model each task by a generative model of the environment. In this work, for simplicity, we only model the current observation. The current task is modelled as a categorical context  $c$  which is treated as the hidden variable in an Hidden Markov Model that explain observations. In such a model the probability of being in a particular context  $c$  at time  $t$  evolves according to:

$$p(c, t+1) = \sum_{c'} p(c', t) \Gamma(c, c')$$

$$\Gamma(c, c') = \delta(c, c')(1 - \alpha) + (1 - \delta(c, c'))\alpha$$

where  $\delta$  is the Kronecker delta function and  $\alpha$  is the probability of switching context. The task context then conditions a generative model predicting the observation probability  $p(o|c, t)$ . Given such generative models, the probability of being in a task set at time  $t$  can be inferred by the observations seen so far as:

$$p(c | o_1 \dots o_t) \propto \sum_{c'} \Gamma(c, c') p(c', t-1) p(o|c, t)$$

The maximal probability context is then taken to be the current task label.

In our implementation, the generative models consist of factored multinomial distributions explaining the probability of the state of each pixel in the observation space. The model is a parametrized Dirichlet distribution, which summarizes the data seen so far using Bayesian updates. In order to encourage each model to specialize, we train the models as follows. We partition time into windows of a particular width  $W$ . During each window, all the Dirichlet priors are updated with the evidence seen so far. At the end of the window, the model best corresponding to the current task set is selected. Since this model was the most useful to explain the current data, it keeps its prior, while all other priors are reverted to their state at the beginning of the time window. We ensure that one hold-out uniform (*i.e.* uninitialized) Dirichlet-multinomial is always available. Whenever the hold-out model is selected a new generative model is created and a new task context is therefore created. This model is Bayesian, in the sense that data is used to maintain beliefs over priors on the generative models, and is non-parametric, in the sense that the model can grow in function of the observed data. It can be seen as an implementation of the flat forget me not algorithm described in [Kieran et al., 2016]. The parameter  $\alpha$  is not learnt. Instead we use the result from [Veness et al., 2012] where it is shown that a time decaying switch rate  $\alpha = 1/t$  guarantees good worst case asymptotic perfmance provided the number of tasks grows as  $o\left(\frac{n}{\log n}\right)$ .

Table 2 summarizes all hyper-parameters used for the Atari experiments. Except for the parameters pertaining the EWC algorithm (Fisher multiplier, num. samples Fisher, EWC start) or pertaining the task recognition models (model update period, model downscaling and size window), all the parameters values are the same as from [van Hasselt et al., 2016] and have not been tuned for these experiments.

Hyperparameter	value	brief description
action repeat	4	Repeat the same action for four frames. Each agent step will occur every fourth frame.
discount factor	0.99	Discount factor used in the Q-learning algorithm.
no-op max	30	Maximum number of do nothing operations carried out at the beginning of each training episode to provide a varied training set.
max. reward	1	Rewards are clipped to 1.
scaled input	84x84	Input images are scaled to 84x84 with bilinear interpolation.
optimization algorithm	RMSprop	Optimization algorithm used.
learning rate	0.00025	The learning rate in RMSprop.
max. learning rate	0.0025	The maximum learning rate that RMSprop will apply.
momentum	0.	The momentum used in RMSprop.
decay	0.95	The decay used in RMSprop.
clip $\delta$	1.	Each gradient from Q-learning is clipped to $\pm 1$ .
max. norm	50.	After clipping, if the norm of the gradient is greater than 50., the gradient is renormalized to 50.
history length	4	The four most recently experienced frames are taken to form a state for Q-learning
minibatch size	32	The number of elements taken from the replay buffer to form a mini-batch training example.
replay period	4	A mini-batch is loaded from the replay buffer every 4 steps (16 frames including action repeat).
memory size	50000	The replay memory stores the last fifty thousand transitions experienced.
target update period	7500	The target network in Q-learning is updated to the policy network every 7500 step.
min. history	50000	The agent will only start learning after fifty thousand transitions have been stored into memory.
initial exploration	1.	The value of the initial exploration rate.
exploration decay start	50000	The exploration rate will start decaying after fifty thousand frames.
exploration decay end	1050000	The exploration rate will decay over one million frames.
final exploration	0.01	The value of the final exploration rate.
model update period	4	The Dirichlet model is updated every fourth step.
model downscaling	2	The Dirichlet model is downscaled by a factor of 2, that is an image of size 42x42 is being modelled.
size window	4	The size of the window for the task recognition model learning.
num. samples Fisher	100	Whenever the diagonal of the Fisher is recomputed for a task, one hundred mini-batches are drawn from the replay buffer.
Fisher multiplier	400	The Fisher is scaled by this number to form the EWC penalty.
start EWC	20E6	The EWC penalty is only applied after 5 million steps (20 million frames).

Table 2: Hyperparameters for each of the MNIST figures

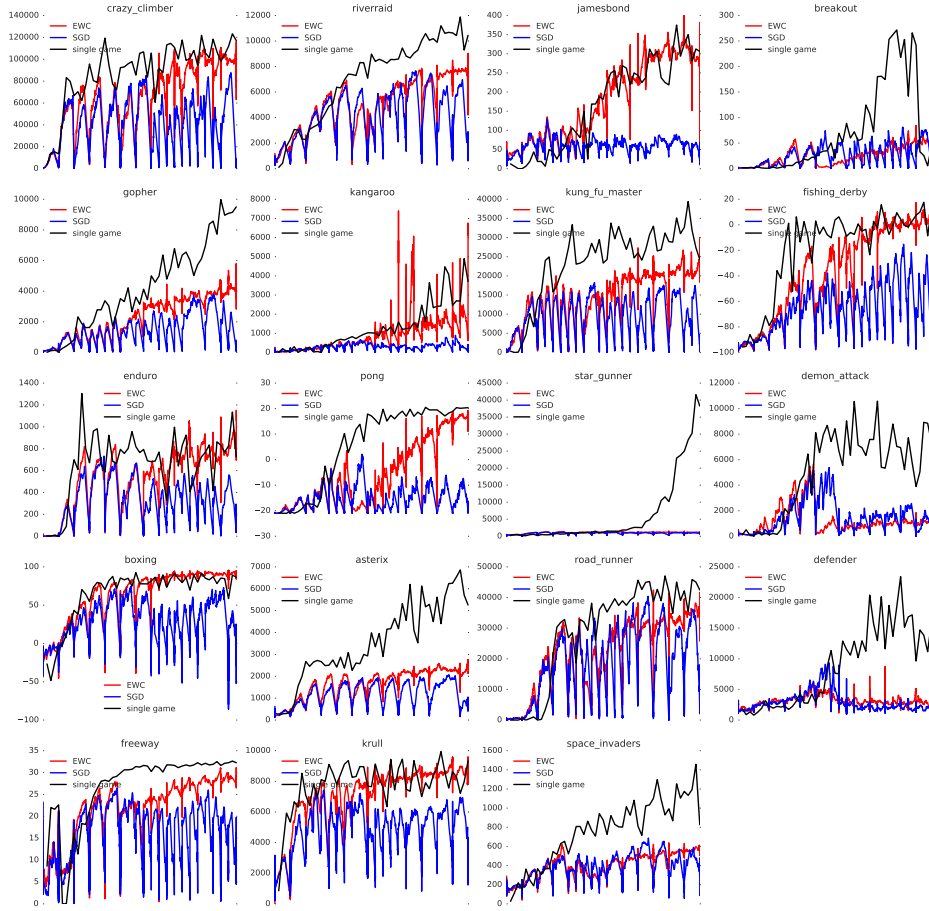


Figure 4: Score in the individual games as a function of steps played in that game. The black baseline curves show learning on individual games alone.

### 4.3 Fisher overlap

To assess whether different tasks solved in the same network use similar sets of weights (Figure 3C in the main text), we measured the degree of overlap between the two tasks' Fisher matrices. Precisely, we computed two tasks' Fishers,  $F_1$  and  $F_2$ , normalized these to each have unit trace,  $\hat{F}_1$  and  $\hat{F}_2$ , then computed their Fréchet distance, a metric on the space of positive-semidefinite matrices [Dowson and Landau, 1982]:

$$\begin{aligned} d^2(\hat{F}_1, \hat{F}_2) &= \frac{1}{2} \text{tr} \left( \hat{F}_1 + \hat{F}_2 - 2(\hat{F}_1 \hat{F}_2)^{1/2} \right) \\ &= \frac{1}{2} \|\hat{F}_1^{1/2} - \hat{F}_2^{1/2}\|_F^2 \end{aligned}$$

which is bounded between zero and one. We then define the overlap as  $1 - d^2$ , with a value of zero indicating that the two tasks depend on non-overlapping sets of weights, and a value of one indicating that  $F_1 = \alpha F_2$  for some  $\alpha > 0$ .